

Flatness Measurement of Semiconductor Wafers Based on Frequency Scanning Interferometry

Weisheng Cheng¹, Xuanzong Wu¹, Zexiao Li¹, Bo Zhang¹, Shuangxiong Yin² and Xiaodong Zhang^{1, #}

¹ State Key Laboratory of Precision Measuring Technology & Instruments, Laboratory of Micro-nano Manufacturing Technology, Tianjin University, Tianjin 300072, China

² Standard Optics Technology Tianjin Co., Ltd. Tianjin 300072, China

Corresponding Author / Email: Zhangxd@tju.edu.cn

KEYWORDS: Frequency scanning interference, Semiconductor chip, Flatness.

Silicon (Si) and Silicon Carbide (SiC), as second and third-generation semiconductor materials, exhibit superior properties that make them highly suitable for high-temperature, high-voltage, and high-frequency applications. However, Si/SiC wafers are characterized by their thinness, high hardness, and brittleness, leading to significant challenges in the production process due to wafer warping and bending, which critically affect subsequent processing. Hence, the ability to rapidly, accurately, and comprehensively monitor and control the thickness, thickness variation, and flatness (including bow and warp) of SiC/Si wafers is a recognized challenge in the industry. To address these challenges, we have developed a frequency scanning interferometry-based system for measuring the flatness of semiconductor thin films. We propose a surface reconstruction algorithm based on an improved least-squares iterative method, identifying error sources such as harmonics and phase shifts, and enhancing the multilayer iterative optimization model to improve the accuracy and robustness of interferometric measurements. Additionally, we introduce the feasibility of an "oversampling" technique for semiconductor wafer measurements, enabling enhanced extraction of weak interference signals from multilayer structures. This approach mitigates the impact of multilayer surface harmonic aliasing on surface reconstruction, achieving high-precision, full-wafer, simultaneous measurement of both surfaces and thickness variations for different semiconductor materials. This paper further discusses the application and advantages of frequency scanning interferometry in measuring the thickness, thickness variation, and flatness of SiC/Si semiconductor wafers. It also explores the effects of different material properties and transmittance on the performance of frequency scanning interferometry.

1. Introduction

Gallium Nitride (GaN) and Silicon Carbide (SiC), as third-generation semiconductor materials, offer distinct advantages in high-power, high-frequency applications due to their wide bandgap, high breakdown field, thermal conductivity, fast electron saturation, and radiation resistance. These properties allow them to operate stably under extreme conditions, making them ideal for high-voltage and high-frequency devices. The rapid growth of the semiconductor industry, particularly driven by automotive electrification and intelligent vehicle technology, has led to increased demand for these materials in smart chips and power semiconductors. In the military sector, their superior performance makes them essential for core electronics in radar and other key equipment.

However, SiC wafers present significant manufacturing challenges, including high costs, difficulty in controlling crystal quality, warpage, bending, surface roughness, and epitaxial growth. Warpage and bending are particularly problematic, impacting subsequent processing and device performance. Accurate measurement of wafer flatness and thickness is crucial to mitigate these issues.

To address this, frequency scanning interferometry has emerged as a preferred method due to its high accuracy, full-width, non-contact, and high-speed measurement capabilities. This technique,

combined with an improved least-squares iterative algorithm and an "oversampling" method, enhances the separation and reconstruction of surface information, allowing for precise measurement of both surface and thickness variations across the entire wafer. Despite these advances, challenges remain in improving measurement accuracy and minimizing errors from fringe aliasing and low contrast.

2. Measurement system structure and method.

2.1 Interferometry system components

The frequency scanning interferometry system comprises a Fischer interferometric optical path, a high-resolution near-infrared camera, an optical alignment camera, a wafer suction cup, an adjustable suction cup stage, a marble support platform, and a computer. This system integrates advanced optical measurement with precise mechanical control for accurate multi-surface profiling of semiconductor wafers.

At its core, the Fischer optical path controls beam splitting and utilizes interference effects to capture fine surface details. The high-resolution near-infrared camera ensures accurate data acquisition with high sensitivity and low noise, while the optical alignment camera maintains the stability of the interferometric path.

The wafer suction cup, with ultra-fine hole vacuum adsorption and flatness better than $2\ \mu\text{m}$, secures 8-inch wafers uniformly. The adjustable stage optimizes the wafer's angle for precise measurements, and the marble platform minimizes environmental vibration, ensuring measurement accuracy.

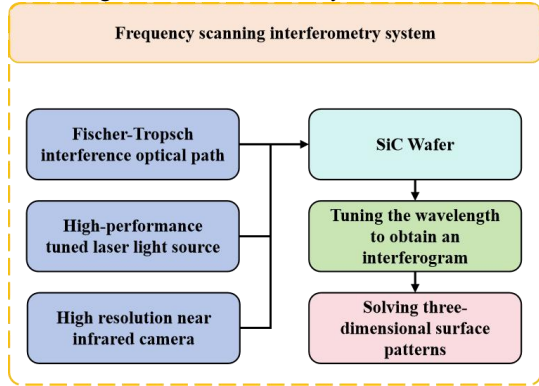


Fig. 1 System structure and world coordinate system.

The laser beam is transmitted through a fiber optic coupler to the interferometer, where a diffusion element optimizes coherence and illumination uniformity. The beam splitter directs part of the beam to the reference mirror and the rest to the wafer as test light. The reflected test and reference light generate interference fringes at the beam splitter, captured by a high-resolution camera and processed by a computer. An algorithm separates signals from each surface, reconstructing the wafer's 3D shape and outputting key parameters such as thickness variation (TTV), thickness (THK), bow (BOW), and warpage (WARP), in compliance with SEMI standards.

2.2 interferogram simulation

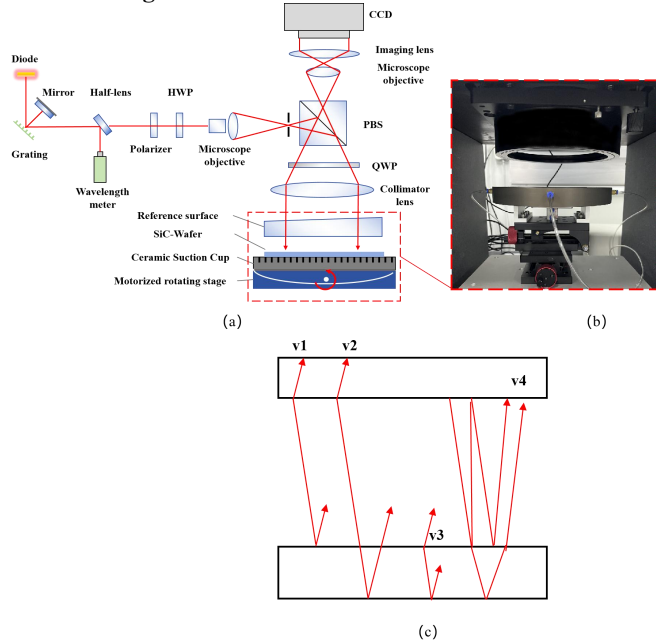


Fig. 2 Schematic diagram of three-surface interference. (a) Interferometry system optical circuit diagram. (b) Measurement modules. (c) Three surface measurement schematic.

When using frequency scanning interferometry for measurements of parallel flat plates, phase information needs to be recovered

from the interferogram in order to obtain three-dimensional topographic information of the measured surface. If the mixed interferometric signal is considered as a superposition of the interference effects of different reflected beams, the expression for the interferometric light intensity at point (x, y) in the interferogram can be transformed into:

$$I(t) = A_0 \left[1 + \sum V_i \cos(\varphi_i - 2\pi\nu_i t) \right] \quad (1)$$

where $\nu_i = 2h_i \Delta\lambda / \lambda$ is the frequency of light intensity change of the interference signal. For multi-surface interference, the frequency of change of light intensity of the interference signal formed by each surface can be written as:

$$\nu_{p,q} = \frac{2\Delta\lambda}{\lambda_0^2} \left[ph + qn_0 T \left(1 - \frac{\lambda_0}{n_0} \frac{dn}{d\lambda} \right) \right] \quad (2)$$

Where p and q denote the number of reflections between the reference mirror and the test mirror, and within the flat plate, respectively; n_0 is the refractive index at wavelength λ_0 . T is the thickness of the flat plate; and $dn/d\lambda$ represents the rate of change of the refractive index with wavelength. ν_1 , ν_2 , and ν_3 correspond to the frequencies of interference formed between the front surface, rear surface of the parallel plate, and the optical thickness variation of the plate, respectively.

$$\nu_1 = \frac{2h\Delta\lambda}{\lambda_0^2} \quad (3)$$

$$\nu_2 = \frac{2(h + nT)\Delta\lambda}{\lambda_0^2} \quad (4)$$

$$\nu_3 = \frac{2nT\Delta\lambda}{\lambda_0^2} \quad (5)$$

$\nu_4 \sim \nu_9$ represent the parasitic signals generated by the remaining multiple reflections in addition to the three surfaces interfering with each other. Under the condition that the refractive index of each point of the parallel plate to be tested is the same, the relative amplitude and frequency distribution of each interference signal are shown in the following table:

Table 1 Distribution of each amplitude and frequency of the three-surface interference signal at $n_0T/h = 3$ (reflectivity $R = 0.04$ for BK7)		
Frequency Component	Relative Amplitude	Frequency Ratio (ν_k / ν_1)
ν_1	1 (fundamental)	1 ($p = 1, q = 0$)
ν_2	1	3 ($p = 0, q = 1$)
ν_3	1	4 ($p = 1, q = 1$)
ν_4	R	2 ($p = 2, q = 0$)
ν_5	R	2 ($p = -1, q = 1$)
ν_6	R	5 ($p = 2, q = 1$)
ν_7	R	6 ($p = 0, q = 2$)
ν_8	R	7 ($p = 1, q = 2$)
ν_9	R	8 ($p = 2, q = 2$)

On the basis of the above double-surface interferometry simulation, and also to ensure the simulation effect, control $h \approx 3n$

$T, n = 1.5$, $dn/d\lambda = 1.5e-13$, and the number of simulation images is 1000. The simulation results are as follows

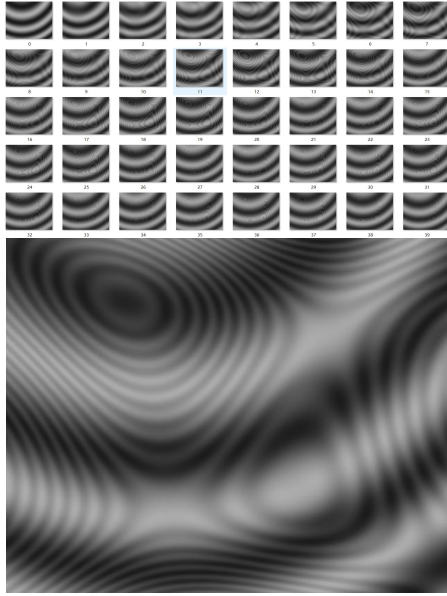


Fig. 3 Simulation of three-surface interference fringes

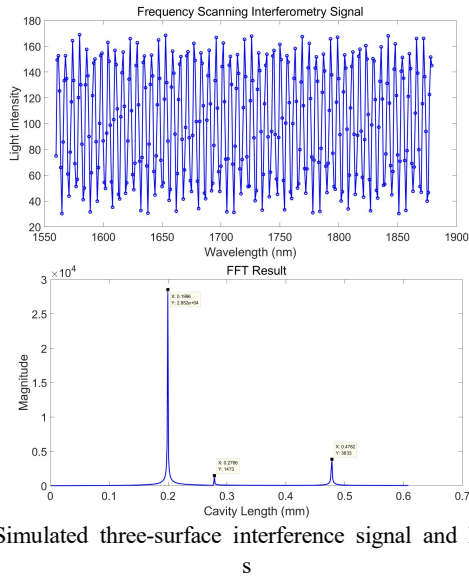


Fig. 4 Simulated three-surface interference signal and FFT result

2.3. Facet Reconstruction Algorithm

To accurately resolve the target phase in multilayer surface interferometry of transparent thin films, this study introduces an innovative method combining harmonic analysis with iterative phase decomposition. Traditional wavelength-tuned interferometry often encounters measurement errors due to harmonic interference from multiple reflections and nonlinear phase modulation. To address this, we propose an iterative phase analysis method based on harmonic decomposition, optimizing the extraction of the target phase by first decomposing the intensity signal into its harmonic components. This approach not only identifies the target phase but also effectively suppresses interference from multiple reflections, enhancing measurement accuracy. Additionally, we refine the partial least squares iterative optimization by incorporating a compensation mechanism for nonlinear phase modulation, reducing its impact on thickness assessment. By dynamically adjusting

the weighting coefficients in the partial least squares model, the algorithm's sensitivity to signal variations is improved, enabling precise multi-surface phase resolution. To further enhance target phase recognition, we utilize five interferometric images, increasing algorithm robustness, suppressing second-order harmonics, and reducing noise from multiple reflections.

$$I_{gh} = S_{gh0} + \sum_{i=1}^R S_{ghi} \cos(\alpha_{gi} + \varphi_{hi} + \Delta\varphi_{ei}) + G_s \quad (6)$$

Where, S_{gh0} is the DC component, S_{ghi} , α_{gi} and φ_{hi} are the amplitude, the tuning variable and the phase of the i th harmonic, respectively, G_s the fixed nonlinear error of the system, this is assembly induced and can be characterized by a high order polynomial, $\Delta\varphi_{ei}$ is the tuning error therein. The fixed nonlinear error of the system is optimized by measuring a standard flat crystal. After bringing in the nonlinear error, the interferometric images of 100 phase adjustments are split into 2 groups of 50 images each at intervals by oversampling technique, the exact phase adjustment error is calculated by using the partial least squares iterative algorithm, and each surface topography is separated and solved to complete the solution.

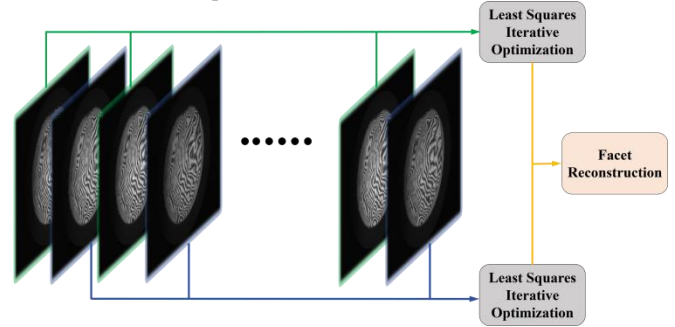


Fig. 5 Over-sampling iterative optimization schematic.

3. Experimental results and discussion

In this paper, experimental tests were conducted on silicon wafers of different materials and wavelength transmittance, covering SiC (substrate wafers), SiC (epitaxial wafers), Si (double-polished wafers), Si (coated wafers), and K9 optical glass. The system is capable of measuring silicon wafers with diameters ranging from 4 inches to 8 inches, and ensures that the measurement time is kept within 2 minutes during single-shot acquisition and solving. Experimental results show a measurement accuracy of 0.05 microns, a repeatability (1σ) of 0.01 microns, and a dynamic thickness measurement range of over 100 microns.

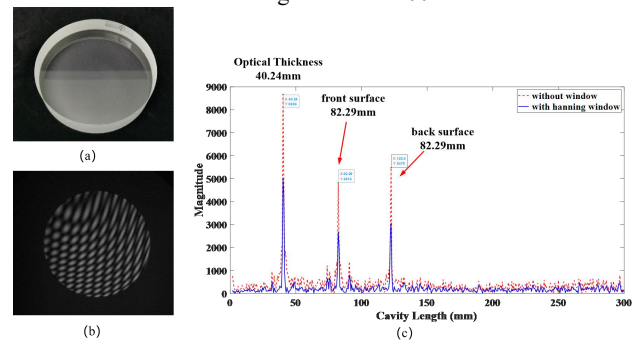


Fig. 6 Flat crystal measurement and fourier spectrum separation.

(a) K9-glass optical flat crystal. (b) Interference figure. (c) Fou
rier spectrogram.

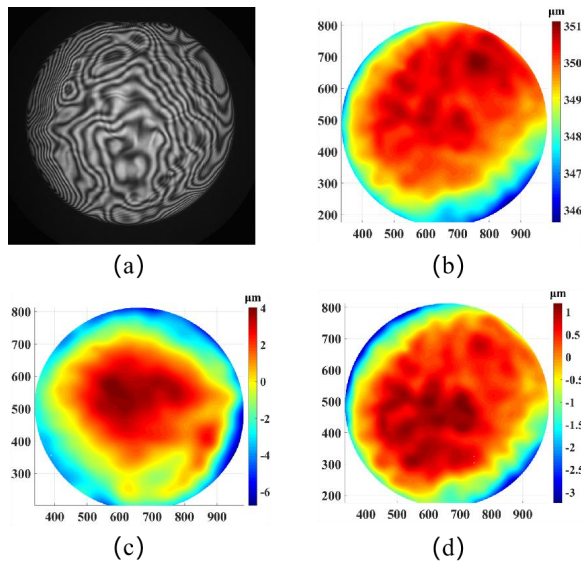


Fig. 7 SiC Product measurement facing process. (a) interference
figure. (b) Back reference. (c) Bow-warp. (d) Median surface.

Table2 Repeatability Measurement Table

number of times	TTV/ μm	Warp/ μm	Bow/ μm
1	5.780	16.481	-5.770
2	5.743	16.639	-5.854
3	5.768	16.649	-5.860
4	5.668	16.662	-5.865
5	5.679	16.664	-5.864
6	5.676	16.666	-5.875
7	5.428	16.676	-5.875
8	5.621	16.663	-5.872
9	5.621	16.670	-5.877
10	5.485	16.671	-5.875
Max Value	5.780	16.676	-5.770
Min Value	5.428	16.481	-5.877
Mean Value	5.647	16.644	-5.859
PV	0.352	0.195	0.107

Table3 Repeatability Evaluation Table

	TTV	Warp	Bow
repeatability (RSD)	2.0%	0.4%	0.5%

In this study, the frequency scanning interferometry system demonstrated high accuracy and stability, with repeatability standard deviations (RSD) of 2.0%, 0.4%, and 0.5% for thickness variation (TTV), warping (Warp), and bowing (Bow), respectively. The system accurately resolves both top and bottom surface facets and reconstructs the full-size multilayer surface topography, pr

oviding 15 flatness parameters, including thickness, TTV, bow, and warp. The measurement results align closely with those from commercial laser interferometry instruments, confirming the system's suitability for comprehensive semiconductor wafer flatness measurements and its significant application potential.

4. Conclusions

This study introduces several innovative improvements for flatness measurement of Si and SiC semiconductor wafers. First, we enhanced the traditional least-squares iterative algorithm to correct harmonic and phase shift errors, significantly boosting measurement accuracy and stability. Second, the introduction of the "oversampling" technique effectively addresses harmonic overlapping on multilayer surfaces, improving the extraction of weak interferometric signals. Finally, by integrating system design with algorithm optimization, the system enables simultaneous measurement of both wafer sides and thickness variations, quickly and accurately determining key parameters like thickness, thickness variation, bow, and warpage. These advancements enhance measurement accuracy, efficiency, and provide robust support for inspecting complex semiconductor materials.

ACKNOWLEDGEMENT

This work is supported by National Natural Science Foundation of China (62373274).

REFERENCES

- Kim S, Kim Y, Hibino K, et al. Interferometric thickness assessment of optical flat by combining iterative analysis and wavelength tuning[J]. Optik, 2022, 265: 169450.
- Sun T, Zheng W, Yu Y, et al. Determination of surface profiles of transparent plates by means of laser interferometry with wavelength tuning[J]. Optics and Lasers in Engineering, 2019, 115: 59-66.
- Dunn T J, Lee C A, Tronolone M J. Frequency stepping interferometry for accurate metrology of rough components and assemblies[C]. Interferometry XV: Techniques and Analysis. SPIE, 2010, 7790: 172-180.